ECCOMAS Congress 2016
VII European Congress on Computational Methods in Applied Sciences and Engineering
M. Papadrakakis, V. Papadopoulos, G. Stefanou, V. Plevris (eds.)
Crete Island, Greece, 5–10 June 2016

MONITORING AND ANALYSIS OF STRESS FIELD FOR ORTHOTROPIC STEEL DECK OF DASHENGGUAN YANGZTE RIVER BRIDGE (ECCOMAS CONGRESS 2016)

Y. Wang[1], Y.S. Song[2]

[1] Jiangsu Key Laboratory of Engineering Mechanics, Southeast University
2# Sipailou Rd., Xuanwu District, Nanjing 210096, China
Civil_wangying@seu.edu.cn

[2]Jinling Institute of Technology,
99 Hongjing Avenue, Jiangning District, Nanjing 211129, China
646814724@qq.com

Keywords: Stress Field, Fatigue Life, High-speed Railway Bridge, Structural Health Monitoring

Abstract: *Driving security of trains with high speed is one of pivotal issues influenced by the smoothness of rail lines significantly. For high-speed railway steel bridges, fatigue cracking of typical positions under the rail lines will reduce stiffness of the deck plate inducing the smooth of the rail lines. In this paper, the strain data recorded by the structural health monitoring system is analyzed and a new theoretical approach is proposed by integrating fatigue assessment of typical welded joint for high-speed railway steel bridge in service. The theoretical approach includes various factors including stress concentration, environmental corrosion and train flow. Having applied in an actual high-speed railway bridge –Dashengguan Yangzte River Bridge, the approach was converted to conduct determinative and reliable fatigue-life evaluation of the bridge. Static-load experiment was conducted to obtain the stress distribution around the weld, as well as the distinction of stress between the positions of weld and strain gauge. The influence of environmental corrosion was integrated by two aspects: increase of stress and reduce of the fatigue resistance. Without consideration of train-weight growth, in conclusion, the fatigue life of typical welded joint will be infinite even if the train flow is with growth constantly. In addition, fatigue life of typical welded joints, determinative or reliable, may be less than the designed service period when growth rate of the train weight arrives at 5%.*

1 INTRODUCTION

High-speed train emerges to satisfy passengers' need of shorter time between distant cities. Trains in high speed are likely to suffer cruel accidents resulting in mayor loss of life and property [1,2]. A mayor concern about the railway transportation system is whether these as-built high-speed railway bridges are robust enough to carry the ever-increasing transportation. Considerable railway bridges were built in steel for lighter weight and easier construction [3,4]. However, steel material and structure are vulnerable to suffering corrosion and fatigue issues especially in welded positions. Thus, subjected to repeated load with ever increasing, there is an urgent need to assess the fatigue performance, remaining fatigue life or reliability combining environmental corrosion.

Fatigue performance assessment requires actual information on structural response of strain at welded position [5-7]. Although Structural Health Monitoring System (i.e. SHMS) has provided strain historical information, proper consideration has to be given involving stress concentration in welds, environmental corrosion and consistent growth of train flow in the future [8,9]. Limited by the feasible positions for strain gauges, measured strain data is incapable of acquiring the strain closing to the weld. So, laboratory test has to be conducted to obtain the stress field around the weld, solving the problems of distinction between the in-situ measurement and actual stress state. In addition, various investigations have been conducted on reduce of cross section by environmental corrosion. But, it is not remarkable to consider the influence of corrosion on fatigue resistance of steel material.

Besides the determinative fatigue-life evaluation of welded joints, reliable fatigue-life evaluation has become much more noticeable, with the growing attention on uncertainty of material, geometry, environmental and loading actions [10,11]. Because of the variation of influencing factors with time, time-dependent reliability assessment becomes essential for full-cycle evaluation of fatigue performance [12]. SHMS has been proved to be one of essential measures to conduct reliability evaluation for actual projects [13]. However, additional investigations require being carried out for the restriction of sensor-system scale and environmental conditions. Mechanical-property and material-resistance experiments are likely to help completion and improvement for the in-situ evaluation of projects.

In this paper, a new theoretical approach is proposed by integrating fatigue assessment of typical welded joint for high-speed railway steel bridge in service. The approach is developed by considering multiple influencing factors - stress concentration, environmental corrosion and growth of train flow. Structural health monitoring system is introduced to provide essential data for fatigue evaluation. Static-load experiment is adopted to obtain the information of stress concentration between the welds and strain-sensor locations. In addition, the relation of the stress reducing and environmental corrosion is derived to coincide with the actual property of plate structure. Finally, determinate and reliable fatigue-life evaluations are conducted by adopting the recommended approach, applying to a large high-speed railway bridge – the Dashengguan High-speed Railway Bridge in China.

2 STRAIN MONITORING SYSTEM OF DASHENGGUAN HIGH-SPEED RAILWAY BRIDGE

Dashengguan High-speed Railway Bridge (Fig. 1 (a))is located in Nanjing city of Jiangsu province in China, spanning the Yangtze River which is the longest river in China. Two national railway lines were conducted and run through the bridge. These two railway lines are respectively Beijing-Shanghai High-Speed Railway and Shanghai-Hankou-Chengdu Railway

and the design speed is 300 km/h and 250km/m. Two kinds of trains serve for these two main rail lines with respectively and 16 carriages. As one kind of steel trussed arch bridge, the vertical view of the bridge is presented in Fig. 1(b) with the main span of 336m. To obtain higher stiffness reducing the risk of train derailing, orthotropic steel deck is applied with internal crossbeams distributed longitudinally.

To acquire structural performance of the railway bridge, structural health monitoring system was installed in construction period. Strain gauges were equipped near rib-to-deck-joint locations for further evaluation of fatigue performance as the orthotropic steel deck is prone to fatigue cracking. The locations of strain gauges are shown in Fig. 1(c). There are two strain gauges in the middle cross section of orthotropic steel deck, which are labeled as DYB-11-23 and DYB-11-24. The strain gauge DYB-11-23 belongs to the side of Beijing-Shanghai High-Speed Railway and DYB-11-24 is on the side of Shanghai-Hankou-Chengdu Railway.

Fig. 1(a) Landscape of the whole bridge

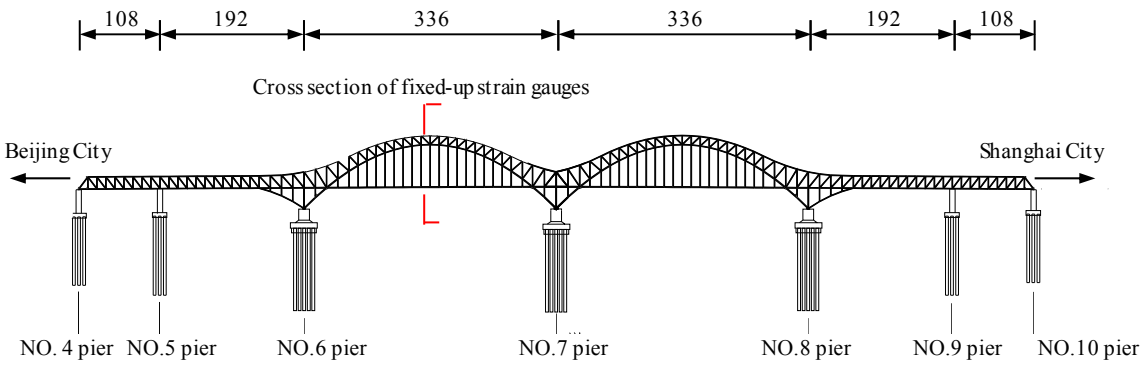

Fig. 1(b) Side elevation of the main bridge (unit: m)

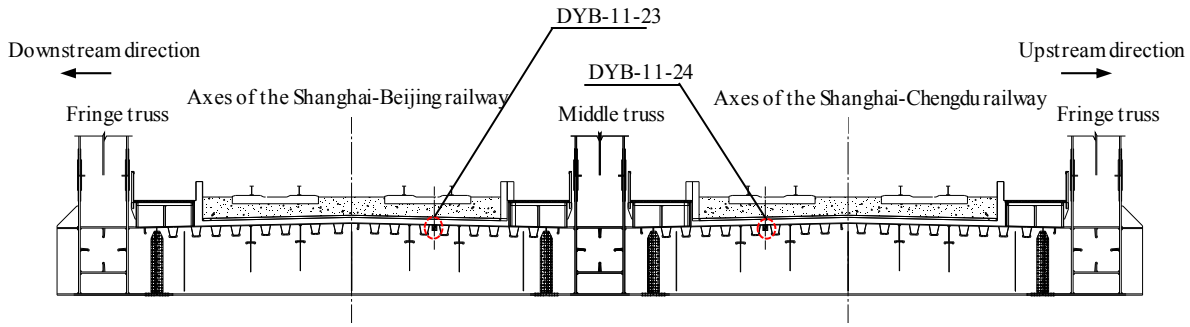

Fig. 1(c) Cross-section diagram of strain gauges

Fig. 1: Layout diagram of strain gauges for steel deck

3 MONITORED STRAIN DATA AND TWO CALCULATED FATIGUE EFFECTS

3.1 Strain history curve under typical trains

In this paper, strain history data is introduced for fatigue evaluation from February to July in 2013. It is presented by Fig. 1 (c) that the strain-gauge locations of DYB-11-23 and DYB-11-24 are symmetrical. Thus, the monitored strain data of DYB-11-24 was merely applied to conduct fatigue analysis. Fig. 2 presents two typical strain history curves of DYB-11-24 under single train. These two curves were induced by typical trains with respectively 8 and 16 carriages. The maximum value of changes in strain is within 2-6 με during the passing of train with8 and 16 carriages. For the train with 8 carriages, the number of the strain peaks is 16 while the same value for the train with 8 carriages is about 32. Considering the number of wheels for each carriage is 2, the number of the strain peaks corresponds to the number of total wheels.

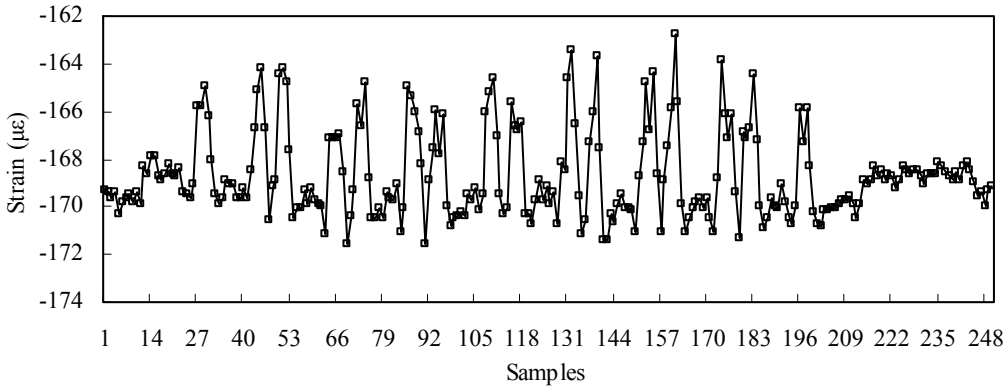

Fig. 2 (a) Typical strain history curve during the passing of train with 8 carriages

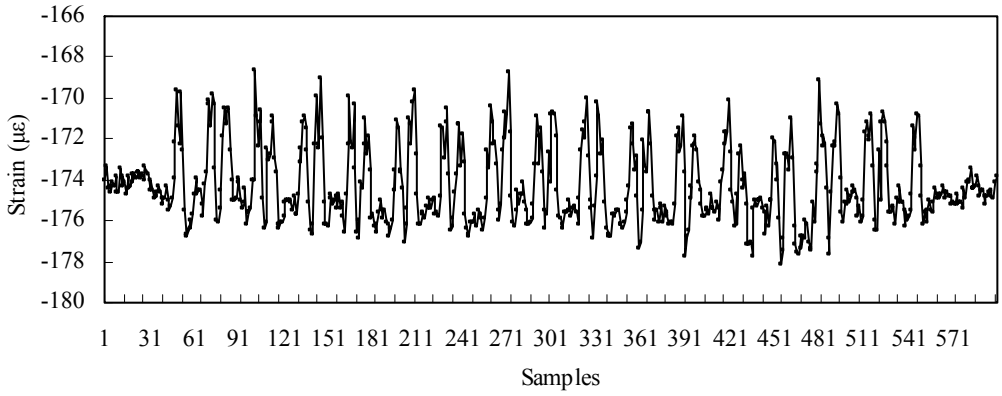

Fig. 2(b) Typical strain history curve during the passing of train with 16 carriages

Fig. 2: Typical strain history curves of strain gauge DYB-11-24 during the passing of typical trains

3.2 Stress amplitude and stress cycle number

Firstly, stress curves were obtained by multiplying0.206 to strain data, in which the units of stress and strain are respectively MPa and με. In addition, 0.206 is the value of elastic modulus of steel in unit of GPa. Stress amplitude and stress cycle number are two typical parameters for evaluating fatigue performance of welded joint. Secondly, rain-flow method was introduced to process the calculated stress history data and stress amplitude spectrum was obtained for further investigation. Fig. 3 presents the stress amplitude spectrum of two typical trains with 8 and 16 carriages. In the figure, the scope of stress amplitudes smaller than 0.3MPa occupying the vast majority is induced by interferences with randomness. Thus, the

stress amplitudes smaller than 0.3MPa were eliminated for further calculation conduction. Finally, two fatigue parameters of Seq (equivalent stress amplitude) and Ns (stress cycle number) under single train were calculated as follows based on the Palmgren and Miner theory combined with standard of Eurocode 3:

$$S_{eq} = \left(\frac{n_i S_i^5}{\sum n_i} \right)^{1/5} \tag{1}$$

$$N_s = \sum n_i \tag{2}$$

where Si is the ith stress amplitude, ni is the number of stress cycle corresponding to Si and 1/5 is slope value of logS-logN curve corresponding the scope of stress amplitude in Eurocode 3. Fig. 4 presents the series of fatigue S-N curves recommended by Eurocode 3. In the figure, the type of rib-to-deck joints corresponds to Type 71 with ΔσD equals to 52 MPa.

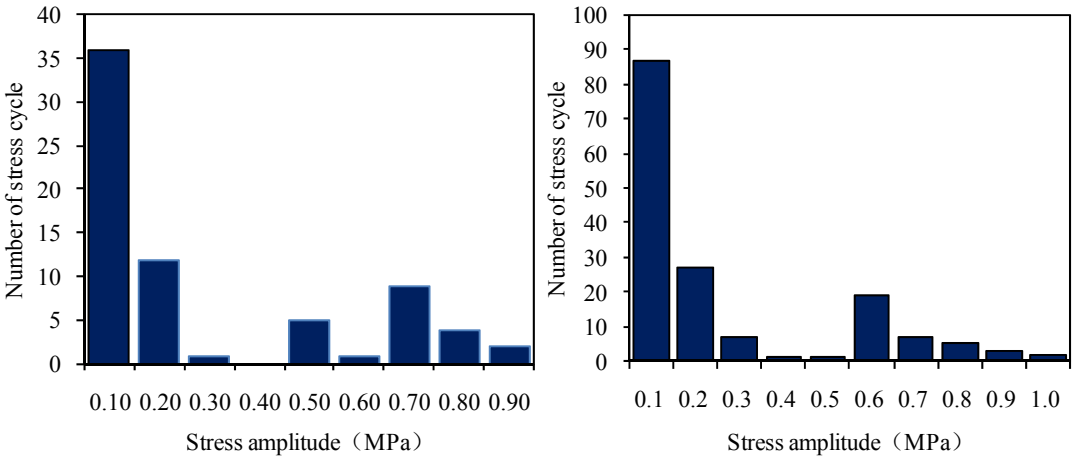

Fig. 3 (a) 8-carriage train Fig. 3 (b) 16-carriage train

Fig. 3: Stress amplitude spectrum of DYB-11-24 under two typical trains

Table 1 presents the calculated results of Seq and Ns for typical stress history curve under single train with 8 and 16 carriages. The values of Seq are similar by comparison of trains with 8 and 16 carriages. The difference ratio between these two trains is only 5.6%. However, the difference of Ns between these two types of trains is much more significant. As the ratio of Ns between two trains is about 2.0, the number of stress cycle is certainly linearly relative with the number of train carriages.

Type of train	***Seq* (MPa)**	***Ns***
8-carriages	0.75	22
16- carriages	0.71	45

Table 1**:** Comparative results of fatigue effects under two typical trains

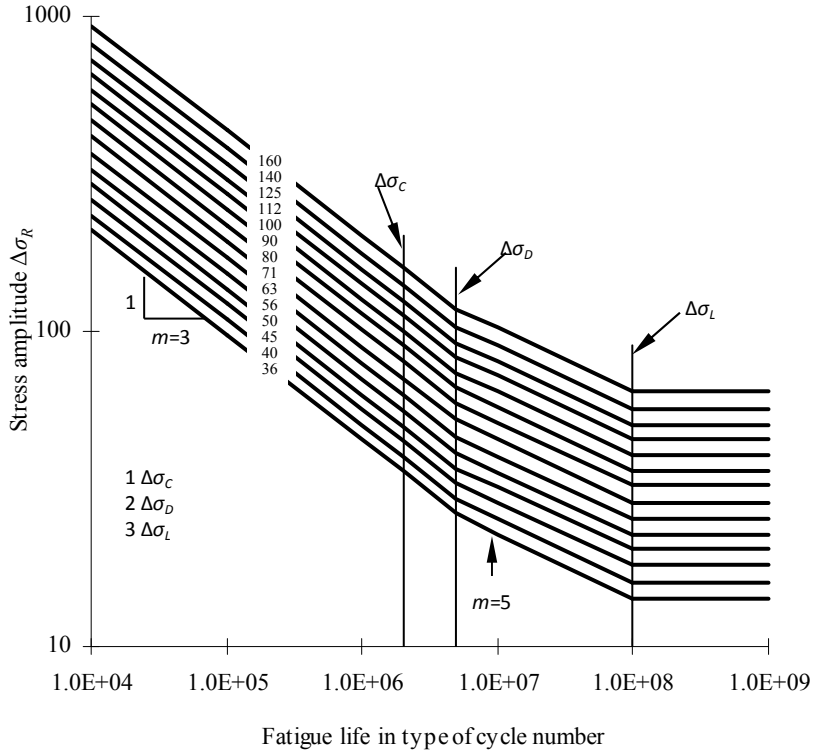

Fig. 4: Series of fatigue S-N curves recommended by Eurocode 3

Time-dependent rule of two fatigue effects is investigated by processing the strain data from February to July in 2013. The processing time unit of the strain data is defined as one day. The treating procedure is similar to presentation in the previous paragraph. Thus, the resultant fatigue effects are so-called daily Seq and daily Ns. Fig. 5 presents the curves of daily Seq and daily Ns from February to July in 2013. The value of daily Seq is similar between various days as the distribution is confined to the scope between 0.67 MPa and 0.80 MPa. However, daily Ns in the first half of the February is much greater than other months. In this period, the train flow is much larger because of the nationally shot rush called Spring Festival Travel in China.

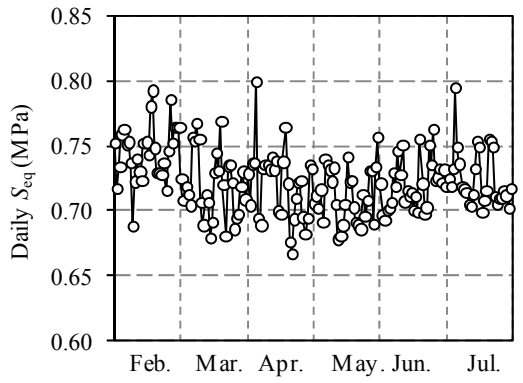

Fig. 5 (a) Daily stress amplitude

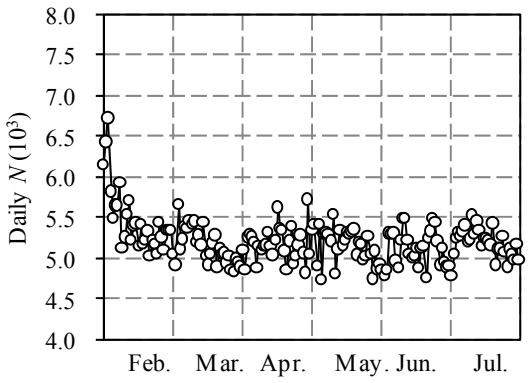

Fig. 5 (b) Daily stress cycle number

Fig. 5: Time-varying curves of two fatigue effects from February to July in 2013

4 MUTI-FACTORS INFLUENCING FATIGUE PERFORMANCE

4.1 Stress concentration

It is presented in the section 3 that the monitored data of strain is capable of obtaining the typical factors accounting fatigue performance. However, accurate evaluation is merely achieved when sufficient causes are taken account into consideration (Ma et al. 2010). Restricted from the field environment and sensor's capability, strain gauges have to be only installed from the weld with certain distance. Thus, the recorded monitoring strain data is much smaller than the actual where approaching the weld toe. Near the weld toe, the stress is called hot-spot stress and the recorded monitoring stress is regard as the nominal stress. Currently, the difference between them is profiled by the parameter called Stress Concentration Factor (SCF) which is described as follows:

$$SCF = S_{hot} / S_{nom} \tag{3}$$

where Shot is hot-spot stress and Snom is nominal stress.

Static-load experiment is conducted to obtain SCF for rib-to-deck welded joint. The geometry of experimental specimen is uniform with actual steel deck of Dashengguan Railway Bridge. The specific dimension of the experimental specimen is presented in Fig. 6 and Table 2. In addition, the WJ-X# indicates the rib-to-deck welded joints of the specimen. Resistance strain gauges are applied to measure the stress distribution around the deck plate under typical load level. The layout of the strain gauges is presented in Fig. 7. The label of DTX and DBX indicates the stain gauges located on the deck top and deck bottom. In addition, the label of RBX indicates the stain gauges on the rib bottom approaching the weld. Typical two-point bending experiment is adopted as static-load mechanism. Fig.8 presents the loading equipment and mechanism for static-load experiments. During the region between the loading points, the bending moment keeps constant and the deck-top/bottom stress at the middle position between neighboring welds is regard as the nominal stress. Then, the stress approaching the weld toe is considered to be the hot-spot stress.

Group	Specimen Number	Deck plate			U-shaped rib				
		Length	Width	Thickness	Opening width	Flange width	Height	Thickness	Spacing
1	OSD1-OSD4	2100	300	16	300	160	280	8	600

Table 2: Typical geometrical parameters of experimental specimen (unit: mm)

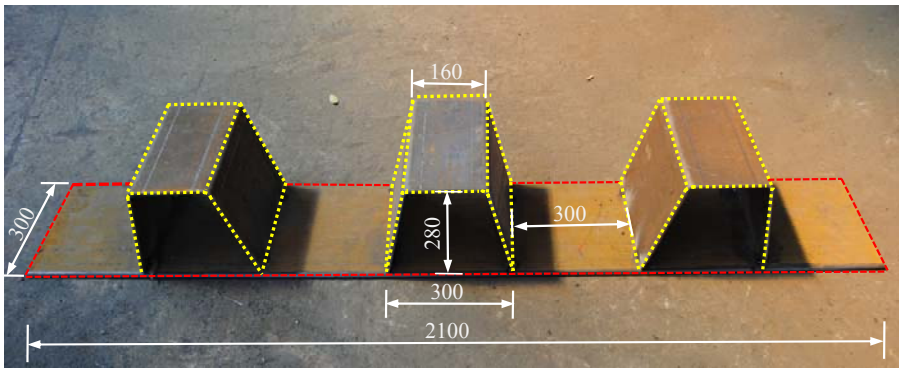

Fig. 6: Geometric parameters of experimental member (unit: mm)

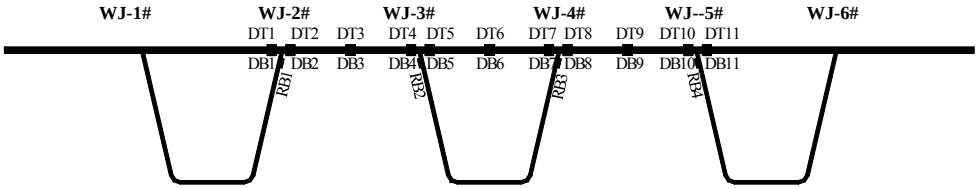

Fig. 7: Layout of strain gauges for experimental specimen

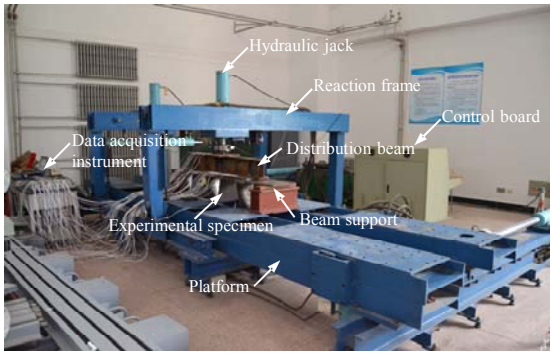

Fig.8 (a) Experimental device of static test

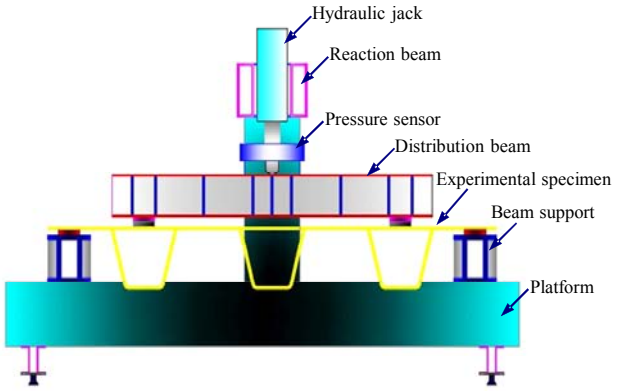

Fig.8 (b) Loading diagram of static test

Fig.8: Experimental diagram of static test for typical experimental specimen

9 load levels are adopted to conduct the static-load experiment. The minimum and maximum loads are 2kN and 18kN with load interval of 2kN. Taking OSD5 for instance, typical stress distribution is presented in Fig. 9 under the loads of 6 kN, 12kN and 18kN. The deck-top stress and deck-bottom stress is similar in absolute value with reverse direction. Thus, the specimen is certainly in the state of the pure moment conforming to the mechanical model. In addition, the stress is nearly equality during the middle region between neighboring welds. However, the stress increases significantly with the locations approaching the welded joint. The SCFs are calculated and obtained by Equation (2). Among the equation, the deck-bottom stress of middle locations between neighboring welds is applied as Snom while the deck-bottom stress approaching the weld toe is adopted as Shot. Various SCFs are presented in Table 3 with two welds for each specimen. It appears that SCFs at different weld location differs significantly because of the distinction from the geometrical dimension of the weld. Thus, fatigue evaluation requires taking into account of the discreteness of SCF.

Specimen	Weld number	Value of SCF	Specimen	Weld number	Value of SCF

number			number		
OSD1	WJ-2#	1.12	OSD2	WJ-2#	1.25
	WJ-3#	1.46		WJ-3#	1.11
	WJ-4#	1.06		WJ-4#	1.55
	WJ-5#	1.32		WJ-5#	1.56
OSD3	WJ-2#	1.11	OSD4	WJ-2#	1.29
	WJ-3#	1.17		WJ-3#	1.13
	WJ-4#	1.11		WJ-4#	1.22
	WJ-5#	1.24		WJ-5#	1.21

Table 3: Data summary of experimental values of SCF around weld toe

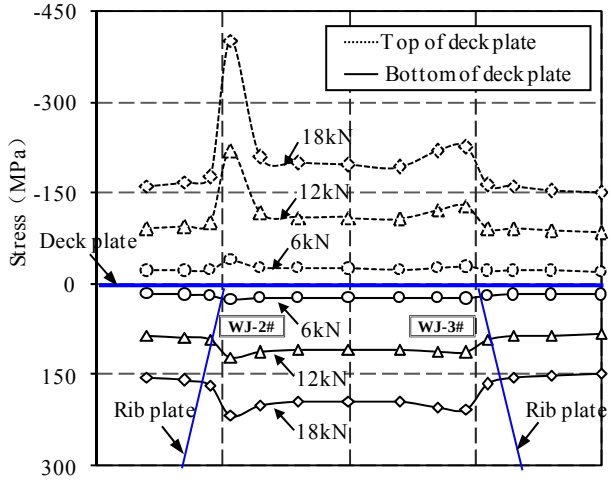

Fig.9: Typical stress distribution of deck plate for OSD 5under various loading steps

4.2 Environmental corrosion

Metal material and structure are subjected to environmental actions such as temperature, wetness and chemical substance in the standing service period [7,8]. Among these causes, fatigue performance of steel structure is affected significantly by the environmental corrosion. The influence of the corrosion is mainly highlighted on two aspects acting on fatigue performance. Firstly, fatigue resistance of steel material degrades gradually under the action of corrosion. Secondly, cross area of steel member decreases with the erosion of the corrosion environment. So, the stress or the stress amplitude magnify with the reducing of the cross area under uniform loads. Thus, above two aspects require taking account into consideration for achieve more accurate evaluation of steel-structural fatigue performance.

Assumptions are proposed to profile the action of corrosion on the cross area. Firstly, depth of the steel plate is merely influenced by the corrosion while the other two geometrical dimensions are consistence with no variation. Secondly, the depth of steel plate is presumed to satisfy the function with time as follows [14]:

$$\delta(t) = bt^r \tag{4}$$

where $\delta(t)$ denotes etch depth of steel plate, tis exposure time of steel structure, b and r is parameters related with material property.

For steel-plate composed structures, stress is influenced more significantly by the etch depth in through-thickness direction. For rib-to deck welded joint belonging to orthotropic steel deck, the stress around deck-plate region is crucial for the performance of fatigue. Previous investigations indicate that flexure stress of deck plate approaching the weld toe is sig-

nificant to fatigue performance. Therefore, the loss rate of section modulus ($\eta(t)$) is described as follows corresponding to the flexure capacity:

$$\eta(t) = \frac{W - \bar{W}(t)}{W} = \frac{2\delta(t)}{B} - \frac{\delta^2(t)}{B^2} \tag{5}$$

where W denotes initial section modulus, $\bar{W}(t)$ is effective section modulus and B is width of cross section.， Bis thickness of steel plate. Assuming the stress is within elastic range around the rib-to-deck joint for deck plate, the bending moment is described as follows:

$$E \cdot \varepsilon \cdot W = E \cdot \bar{\varepsilon}(t) \cdot \bar{W}(t) \tag{6}$$

where E denotes elastic modulus of steel material, ε and $\bar{\varepsilon}(t)$ are initial strain and the strain at time of t respectively.

Substituting equation (5) into (6), then:

$$\bar{\varepsilon}(t) = \frac{1}{1 - \frac{2\delta(t)}{B} + \frac{\delta^2(t)}{B^2}} \varepsilon \tag{7}$$

Finally, effective stress amplitude (S(t)) is described as follows:

$$S(t) = \frac{1}{1 - \frac{2\delta(t)}{B} + \frac{\delta^2(t)}{B^2}} S_n \tag{8}$$

where Sn denotes nominal stress amplitude which is calculated by initial area of cross sections.

Compared to the aggravation of near-weld stress for typical members, material property of fatigue resistance is much harder to profile under the action of environmental. Typical resistance models for fatigue of the specific welded joint are described by series of S-N curves. Most equations corresponding to S-N curves are shown as:

$$\lg N = \lg C - m \lg S \tag{9}$$

where N denotes fatigue life represented by cycle number, C is model parameter relating to material property, m is slop of lg$S$-lg$N$ curves, and S is stress amplitude of welded joints. Plenty of investigations have pointed out that the value of m keeps consistent by action of the environmental corrosion. In addition, the parameter C indicates time-dependent fatigue resistance of steel material acted by corrosion. Thus, C is transferred as $C(t)$ to account for its time-dependent property. Some fitting functions have been proposed to profile the time-dependent property of $C(t)$. In further, exponential function has been recommended for application described as follows [14]:

$$C(t) = C_0 \varphi(t) = C_0 e^{-\alpha t} \tag{10}$$

Where C_0 is initial parameter of welded joint without environmental corrosion, φ(t) is degenerate function of C, and α is fitting parameter of $C(t)$ relative with environment condition and types of welded joints.

5 DETERMINATIVE FATIGUE- LIFE EVALUATIONS INTEGRATING MULTIPLE FACTORS

5.1 Primary evaluation method

Fatigue-resistance model is the basis to conduct fatigue- life evaluation. Typical codes for fatigue evaluation of steel bridge include BS5400, Eurocode 3and AASHTO. Compared to the ancient code of BS5400, Eurocode3and AASHTO involve the influence of stress threshold, which means that fatigue life of typical welded joints is infinite when stress amplitude is less than a certain value. Such kinds of certain value were called fatigue life constant amplitude fatigue limit. In addition, different slope value is taken into account at various scope of stress amplitude. Thus, Eurocode 3 has been applied to conduct the fatigue design and evaluation of steel bridge in mayor nations and regions.

Similarly with typical fatigue-resistance codes, fatigue life profiled by Eurocode 3 in shape of series of *S*-*N* curves. Fig. 4 presents the series of *S*-*N* curves for various types of welded joints. In the figure, $\Delta\sigma_C$ presents type of welded joints defined by constant stress range $\Delta\sigma$R ($\Delta\sigma_R$=2.0×*S*) in condition of stress cycle number equals to two million. $\Delta\sigma_C$ and $\Delta\sigma_L$ denote respectively constant fatigue limit and fatigue cut-off. The value of constant slope m of lg*S*-lg*N* curves equals to zero in condition of $\Delta\sigma_R<\Delta\sigma_L$. In such range, fatigue life of welded joints is infinite. In range of $\Delta\sigma_L\leq\Delta\sigma_R<\Delta\sigma_D$, the value of m varies from zero to five while the value of m becomes three when $\Delta\sigma_R \geq \Delta\sigma_C$.

Fatigue damage requires being calculated and obtained to confirm subsequently the fatigue life of typical welded joint. Plamgren-Miner methodology is adopted in mayor scopes including fatigue design and real-time evaluation. The methodology is based on the assumption of linear damage accumulation described as follows:

$$D = \sum_{S_i \geq \Delta\sigma_D} \frac{n_i S_i^3}{K_C} + \sum_{\Delta\sigma_L \leq S_j \leq \Delta\sigma_D} \frac{n_j S_j^5}{K_D} \tag{11}$$

where K_C and K_D keynote parameters related with types of welded joint.

Suffered from variable stress amplitudes, the most significant issue is how the fatigue life in confirmed by corresponding to the accumulated fatigue damage. Although the linear fatigue-damage methodology of Plamgren-Miner has been admitted widely, the ultimate value of accumulated fatigue damage, which indicates the ultimate fatigue life, is still in dispute. The reason for these disputes is mainly because linear fatigue-damage methodology does not include the nonlinear influence of fatigue damage by variable stress amplitudes. Therefore, fatigue life may achieve when fatigue damage *D* is less or more than 1.0. For simplification, deterministic fatigue life is confirmed and obtained by principle of fatigue damage *D* equaling to 1.0.

5.2 Fatigue-life evaluation considering multiple factors

Having identifying the general principle of evaluating fatigue life, fine factors are then required being taken account including the influence of stress concentration and environmental corrosion. Firstly, influence of stress concentration is represented by SCF. According to the result of static-load experiment, the value of SCF scatters in scope from 1.11 to 1.56. The mean value of SCF equaling to1.24 is adopted to conduct fatigue evaluation for simplification. Secondly, fatigue capacity is reflected in two aspects of $\Delta\sigma_C$ and $\Delta\sigma_L$ described by Equation (10). A is set as 0.006 and C_0 is selected as $\Delta\sigma_L$, $\Delta\sigma_R$, $\Delta\sigma_D$, K_C and K_D.As recommended by Eurocode 3 for rib-to-deck welded joint, $\Delta\sigma$L, $\Delta\sigma_R$,, $\Delta\sigma_D$, K_C and K_D are respectively 70MPa, 52MPa, 29MPa, 7.16×1011 and1.90×1015. Thirdly, the weakness of section corresponding to

corrosion is presented by Equation (4) to (8). In the equation, b and r is made as 60 and 0.48 [14].

Daily Seq is consequently obtained with the increase of service time, presented by Fig. 10. With the growth of service time, the daily S_{eq} increases linearly with the service time. When the service time arrives at 100 year, the daily S_{eq} reaches at 1.04 MPa. Even through the service time arrives at 300 year, three times of the designed service period, the daily S_{eq} is only about 1.09 MPa. Fig. 11 presents curves of $\Delta\sigma L$ decreasing with commission period nonlinearly. $\Delta\sigma_L$ equals to 15.9, 8.7 and 4.8 MPa, when commission period arrives at 100, 200 and 300 years. Without consideration of increase of train weight, Se,d is far less than $\Delta\sigma L$ indicating that fatigue life of rib-to-deck welded joints is beyond 300 years. As the designed service life of bridge is 100 years, fatigue life of orthotropic steel deck of Dashengguan Bridge can be considered infinite.

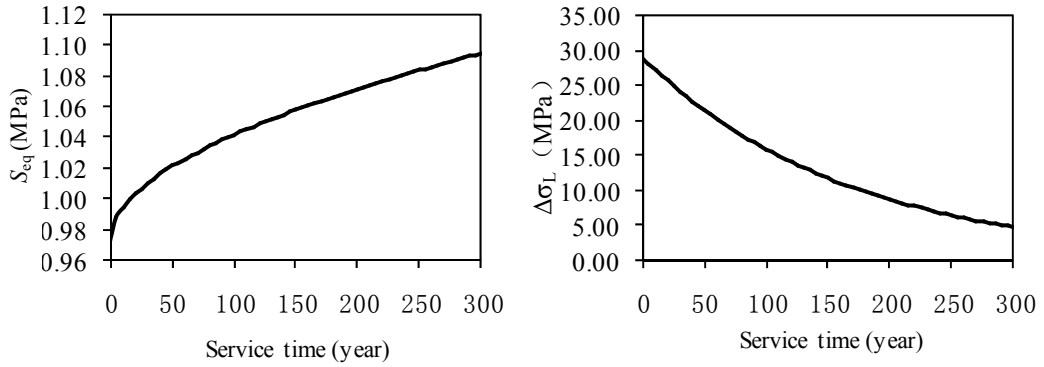

Fig.10: Curve of equivalent stress amplitude with service time Fig.11: Curve of fatigue limit with service time

5.3 Discussion on influence of train weight, train flow and number of carriages

However, fatigue life is perhaps not infinite when taking account of sustained development of train weight. If the stress of orthotropic steel deck is within elastic range under train load actions, the stress amplitude is linearly increased with the growth of train weight. Annual growth rate of train weight is introduced to considering the sustained development of train weight. The value of 1%, 3% and 5% are adopted to investigate the influence of train weight growth on fatigue life. Fig. 12 presents the curves of $S_{e,d}$ under growth rate of train weight of 1%, 3% and 5%, as well as the variation curves of $\Delta\sigma_L$ and $\Delta\sigma_D$. When the train weight is increased by annual growth rate of 1% and 3%, $S_{e,d}$ approaches to $\Delta\sigma L$ at the time of 95th year by far. It indicates that fatigue life is much greater than the designed service period of 100 years.

Yet, $S_{e,d}$ is perhaps beyond $\Delta\sigma_L$ and $\Delta\sigma_D$ at 61th and 72th year when annual growth rate of train weight reaches at 5%.It is known from Equation (11) that there is no fatigue damage within the first 61 years and fatigue damage is accumulated from 61th and index of stress amplitude transform from 5.0 to 3.0 at 72th. Fatigue life is consequently 77 years when accumulated fatigue damage *D* reach at 1.0. It means that fatigue failure perhaps occurs within the designed service life (100 years).

However, above investigations merely includes the increase of train weight without consideration of annual train flow and number of train carriages. If these two factors are taken account of, the calculated fatigue life becomes much shorter, less than 77 years.

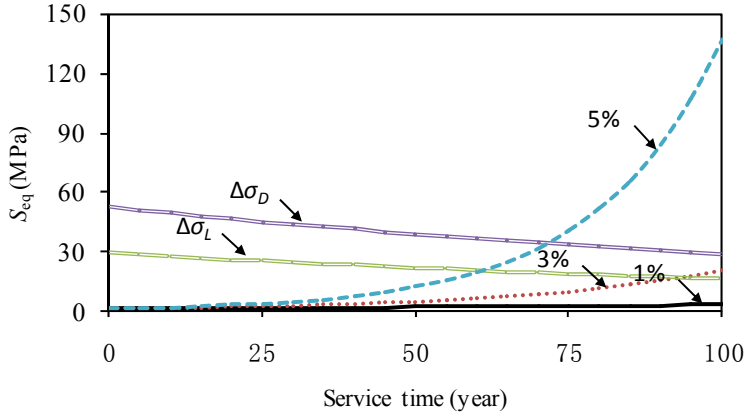

Fig.12: Curves of equivalent stress amplitude, constant-amplitude fatigue limit and cut-off fatigue limit with the service time

6 TIME-DEPENDENT FATIGUE RELIABILITY ASSESSMENT

6.1 Limit state equation of fatigue failure

When stress amplitude exceeds the constant fatigue limit, fatigue damage is accumulated induced by action of sustained train load and environmental corrosion. Fatigue failure perhaps occurs in condition that the fatigue damage arrives at critical value. Thus, the limit state equation of fatigue failure for welded joint can be described as follows:

$$g(X)=\Delta-e\cdot D=\Delta-e\cdot\left(\sum_{S_i\geq\Delta\sigma_D}\frac{n_iS_i^3}{K_C}+\sum_{\Delta\sigma_L\leq S_j\leq\Delta\sigma_D}\frac{n_jS_j^5}{K_D}\right) \tag{12}$$

where△ denotes ultimate value of fatigue damage, e is correction factor caused by error measurement of strain gauges and D is accumulated fatigue damage calculated by Equation (11).

When g(X)<0, the welded joint is under fatigue-failure state in probability sense. Thus, fatigue failure probability is described as $p_f=p(g(X)<0)$ and the fatigue reliability index β is calculated as follows:

$$\beta=\Phi^{-1}(1-p_f)=-\Phi^{-1}(p_f) \tag{13}$$

where $\Phi^{-1}(\cdot)$ denotes inverse function of standard normal distribution.

6.2 Probability-distribution function of critical factors

There are four variables in the fatigue-failure limit state equation, i.e. △, *e*, *Si (Sj)*. Above determinative fatigue-life calculation is based on the assumption that fatigue life arrives when fatigue damage D equals to 1.0. However, fatigue failure may occur when the D is unequal to 1.0 with random distribution. According to related investigation from article [15], e is described statistically as normal distribution whose mean value and standard deviation are respectively 1.0 and 0.03.

Fig. 13 presents the calculated histogram distribution of two fatigue effects, i.e. daily *Seq* and N. In the figure, Nominal, Log-nominal and t-distribution functions are applied for profiling. By contrast, t-distribution function fits much better than the two others. Thus, t-distribution functions are applied to profile statistical property of daily *Seq* and *N*. Table 4 presents the parameters of t-distribution function for daily *Seq* and *N*.

Fatigue effect	Distribution function	Mean value	Standard deviation	Variable cofficient
Daily Seq	t-distribution	0.72	0.025	0.03
Daily N	t-distribution	5179	267	0.05

Table 4. Parameters of probabilistic models for daily S_{eq} and daily N

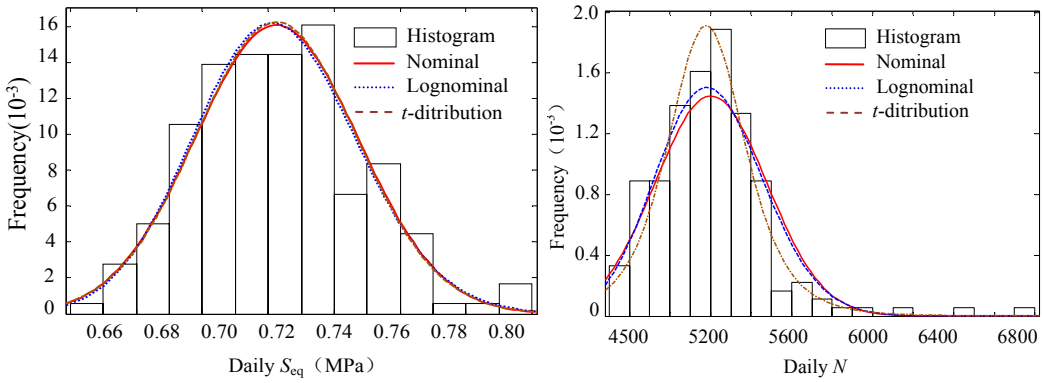

Fig. 13: Probabilistic models of daily equivalent stress amplitude and daily stress cycle number

6.3 Time-variant fatigue-reliability index

Because of the randomness of influencing factors, reliability evaluation is constantly applied to assess in-service performance of engineering structure. With the service time going on, the stochastic behavior of influencing factors varies inducing the transformation of structural reliability. The characteristic of structural reliability corresponding to time is so-called time-dependent reliability.

Constantly, reliability index βis adopted as the parameter for evaluation the reliability. Various methods has been carried out to calculate the reliability index β. These presentative methods include First Order Second Moment Method, Response Surface Method and Monte-Carlo Simulation Method. Typically, Monte-Carlo Simulation Method is much more applicable in situation when influencing factor does not fit the Nominal distribution function. Monte-Carlo Simulation Method conducts random sampling directly based on statistical model of actual events. Then, the occurrence frequency of actual events is acquired such as the fatigue-failure frequency of welded joints.

In this paper, Monte-Carlo Simulation Method is applied to acquire the approximate solution of fatigue failure probability according to Equation (12). Influencing factors are taken account of including the stress concentration, environmental corrosion as well as the growth of train weight. The action rule of above influencing factors is considered by Section 4 incorporating the time effect. Fatigue reliability index β is finally commutated by Equation (12).

The value of 100,000 is selected as the sampling number in each condition for typical Monte-Carlo Simulation process. Including the influencing factors mentioned above, three kinds of growth rate of train weight, i.e. 1%, 3% and 5%, are adopted as typical conditions. Fig. 14 presents the curves of fatigue reliability index β corresponding to time under above three typical conditions. The target reliability index is selected as 3.0 according to engineering experience [16]. In the figure, the fatigue reliability index β maintains 3.30 until the designed service period of 100 years under the condition of growth rate of train weight with 1% and 3%.

In contrast, the fatigue reliability index β maintains 3.30 until the 84th year when the growth rate of train weight equals to 5%. Then, the fatigue reliability index β declines rapidly and reaches 3.0 at the time of 85th year. After short-time volatility for about ten years, the fatigue reliability index β maintains at constant level equaling to 0.0. It indicates that fatigue failure may occur with significantly high probability.

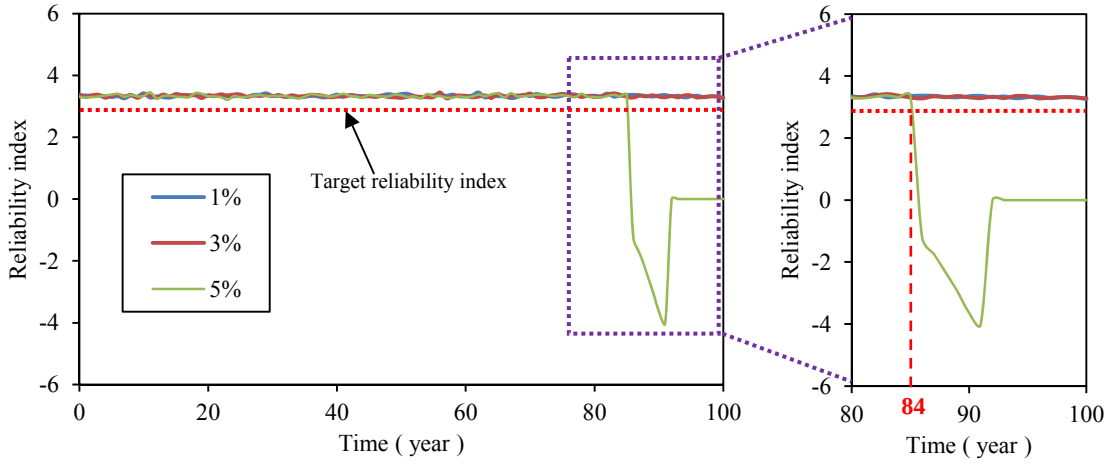

Fig.14: Curve of reliability index with time under different growth rate of train weight

7 CONCLUSIONS

Fatigue issue is typical structural performance for high-speed railway bridge. Once fatigue cracking is happened in the deck plate under rail lines, the ride performance of the high-speed train is reduced inducing potential major traffic accident. Obtained from the structural monitoring system, strain history data provides chances to conduct the real-time fatigue evaluation for typical high-speed railway bridge. In this paper, the fatigue performance is evaluated for Dashengguan High-speed Railway Bridge in China by assessing its fatigue life and time-dependent fatigue reliability. In addition, multiple factors are taken into account including stress concentration, environmental corrosion and growth of train weight. Conclusions are presented as follows:

- Under the passage of trains with different number of carriages, the value of equivalent stress amplitude is approaching with each other. However, the stress cycle number is proportional to the number of train carriages, indicating the linear relation between stress cycle number and train axle number.
- Without consideration of the randomness of influencing factors, the fatigue life of rib-to-deck welded joint is infinite taking only account of environmental corrosion and stress concentration. If consistent development of train weight is considered, the fatigue life may decrease to the value less than the designed service period. For instance, fatigue life is only about 132 years and 77 years when the annual growth rate of train weight reaches to 3% and 5%.
- Similarly to the fatigue-life evaluation without regardless of randomness, fatigue reliability of rib-to-deck welded joint remains at relatively higher level taking no account of the consistent development of train weight. If the growth rate of train weight is considered as 5%, the fatigue reliability index is less than the target reliability index when arriving at the 84th year. Thus, the reliable fatigue life is 84 years when the growth rate of train weight equaling to 5%. Consequently, it indicates that fatigue performance of rib-to-deck welded joint is likely to be unreliable within the design-life period.

ACKNOWLEDGEMENTS

The work described in this paper was substantially supported by the grant from the National Natural Science Foundation of China (No. 51008069), the Priority Academic Program Development of Jiangsu Higher Education Institutions (PAPD), and the Top-notch Academic Programs Project of Jiangsu Higher Education Institutions (TAPP), which are gratefully acknowledged.

REFERENCES

[1] D. Baxter, D. Nemovitz. Sensitivity analysis of rail–structure interaction force effects for direct-fixation, *In Annual Conference & Exposition AREMA*. 2012.

[2] Y. Bin, G.L Dai, and H.P. Zhang, Beam–track interaction of high-speed railway bridge with ballast track, *J Cent S Univ Technol* , 1447–1453, 2012

[3] Z.G. Xiao, K. Yamada, S. Ya, et al. Stress analyses and fatigue evaluation of rib-to-deck joints in steel orthotropic decks. *International Journal of Fatigue,* 1387–1397, 2008.

[4] M.S. Pfeil, R.C. Battista and A.J.R. Mergulhao. Stress concentration in steel bridge orthotropic deck. *J Construct Steel Res,* 1172–1184, 2005.

[5] T. Guo, A.Q. Li, and H. Wang. Influence of ambient temperature on the fatigue damage of welded bridge decks, *International Journal of Fatigue,* 1092-1102. 2008

[6] Y. Wang, Z.X. Li, and A.Q. Li, Combined use of SHMS and finite element strain data for assessing the fatigue reliability index of girder components in long-span cable-stayed bridge, *Theoretical and Applied Fracture Mechanics,* 127-136, 2010

[7] Y.S. Song, and Y.L Ding. Fatigue monitoring and analysis of orthotropic steel deck considering traffic volume and ambient temperature, *Sci China Tech Sci,* 1758-1766, 2013

[8] R. Rahgozar, and Y. Sharlifi. Remaining fatigue life of corroded steel structural members, *Advances in Structural Engineering,* 881-890, 2011

[9] Y.T. Ma, Y. Li and F.H Wang. The atmospheric corrosion kinetics of low carbon steel in a tropical marine environment, *Corrosion Science,* 1796-1800, 2010

[10] X.W. Ye, Y.Q. Ni and J.M. Ko. Experimental evaluation of stress concentration factor of welded steel bridge T-joints, *Journal of Constructional Steel Research,* 78-85, 2012

[11] X.W. Ye, Y.Q. Ni, K.Y. Wong, et al. Statistical analysis of stress spectra for fatigue life assessment of steel bridges with structural health monitoring data, *Engineering Structures,* 166-176, 2012

[12] T. Guo, and Y.W. Chen, Field Stress/Displacement Monitoring and Fatigue Reliability Assessment of Retrofitted Steel Bridge Details, *Engineering Failure Analysis,* 354-363, 2011

[13] A.Q. Li, Y.L. Ding and H. Wang. Analysis and assessment of bridge health monitoring mass data—Progress in research development of “Structural Health Monitoring”, *Sci China Tech Sci,* 2212–2224, 2012

[14] J.X. Gong, and G.F. Zhao. Fatigue reliability analysis for corroded reinforced concrete structures, *China civil engineering journal,* 50-56, 2000

[15] D.M. Frangopol, A. Strauss and S. Kim. Bridge Reliability Assessment based on Monitoring, *Journal of Bridge Engineering,* 258-270, 2008

[16] P.H. Wirsching, and Y.N. Chen, Fatigue design criteria for TLP tendons. *Journal of Structural Engineering,* 1398-1414, 1987.